An Integral Equation To Describe the Solvation of Polar Molecules in Liquid Water

Dmitrii Beglov and Benoît Roux*

Departments of Physics and Chemistry, Université de Montréal, C.P. 6128, succ. Centre-Ville, Canada H3C 3J7, and Centre de Recherche en Calcul Appliqué (CERCA), 5160 Decarie, Montreal, Canada H3X 2H9

Received: March 27, 1997[⊗]

We developed and implemented a statistical mechanical integral equation theory to describe the hydration structure of complex molecules. The theory, which is an extension of the reference interaction site model (RISM) in three dimensions, yields the average density from the solvent interactions sites at all points **r** around a molecular solute of arbitrary shape. Both solute−solvent electrostatic and van der Waals interactions are fully included, and solvent packing is taken into account. The approach is illustrated by calculating the average oxygen and hydrogen density of liquid water around two molecular solutes: water and *N*-methylacetamide. Molecular dynamics simulations are performed to test the results obtained from the integral equation. It is observed that important microscopic structural features of the average water density due to hydrogen bonding are reproduced by the integral equation. The integral equation has a simple formal structure and is easy to implement numerically. It offers a powerful alternative to computer simulations with explicit solvent molecules and to continuum solvent representations for incorporating solvation effects in a wide range of applications.

I. Introduction

Computer simulations of atomic models with explicit water represent the most detailed theoretical approach for studying the influence of solvent on the conformation of complex biological molecules.[1] Nevertheless, these computationally intensive methodologies often suffer from statistical uncertainties due to finite sampling. Computations with explicit solvent molecules become even more intensive if the solute−solvent interactions are treated at an ab initio level.[2,3] Alternatively, it is attractive to capture the dominant solvation effects using approximate representations of the solvent in which the solvent is described implicitly in terms of a continuum. A variety of computational schemes have been developed, such as the Kirkwood−Onsager reaction field,[4,5] macroscopic continuum electrostatics,[6] generalized Born model,[7] conductor boundary conditions,[8,9] and many others (for an extensive review, see ref 10). However, continuum models neglect many essential features of liquid water and are thus seriously limited. In particular, the granularity of the solvent (the fact that it is composed by molecules of finite size), which is an important factor influencing the molecular packing, is ignored in continuum models. Furthermore, the ability of water molecules to form hydrogen bonds with the solute is not taken into account. At the present time there is a need for an intermediate approach that is less computationally expensive than simulations with explicit solvent but that avoids the oversimplifications of the continuum models.

Statistical mechanical integral equation theories of liquids provide a rigorous framework for developing computational approaches describing solvation phenomena.[11] For example, the reference hypernetted chain equation (R-HNC),[12] an advanced integral equation theory, is able to provide detailed information about the positional and orientational pair distribution functions of the solvent around the solute. However, numerical solutions, expressed as an expansion in terms of rotational invariants, are difficult to obtain in the case of large molecular solutes that are markedly nonspherical. Theories based on site−site radial distribution functions such as the reference interaction site model (RISM) equation are computationally simpler.[13] The RISM theory has been used in combination with a site−site HNC closure[13,14] to study the solvation of monoatomic solutes at infinite dilution in liquid water,[15,16] small peptides,[17−21] as well as a large number of organic molecules.[22] However, the theory is not appropriate for large molecular solutes, since completely buried atoms of the solute are only partially shielded from the solvent. Furturemore, the dielectric constant of the pure liquid is not described satisfactorily. There have been several efforts to correct the deficiencies of the theory. For example, a reformulated dielectrically consistent RISM equation was developed to model finite-concentration salt solutions.[23] Nevertheless, because the standard RISM theories are based on a reduction to site−site solute−solvent radially symmetric distribution functions, there is a loss of information about the three-dimensional spatial organization of the solvent density around a nonspherical molecular solute.

Recently, it has been possible to formulate and solve integral equations able to take into account the full distribution of the solvent around solutes of irregular shape in three dimensions.[24−26] The HNC[24] and Percus−Yevick[25] integral equations describing the density of a simple Lennard-Jones solvent around nonpolar solutes of arbitrary shape were solved numerically on a three-dimensional grid. To account for electrostatic interactions, an extension to the mean-spherical-approximation integral equation in three dimensions (3d-MSA) describing the distribution function of a liquid constituted of spherical molecules with an embedded dipole around a polar solute was formulated and solved numerically.[26] Such intermediate approximations can incorporate the essential properties of a polar liquid. For example, it was possible to rigorously demonstrate that the 3d-MSA equation reduces to the Poisson equation used in macroscopic continuum solvation models under specific assumptions.[26] Nonetheless, the representation of water molecules as spherical particles with an embedded dipole is limited because

* To whom correspondence should be addressed. E-mail: rouxb@plgcn.umontreal.ca. Telephone: (514) 343-7105. Fax: (514) 343-7586.

⊗ Abstract published in *Advance ACS Abstracts,* July 15, 1997.

S1089-5647(97)01083-3 CCC: $14.00 © 1997 American Chemical Society

hydrogen bonding is not easily taken into account. Other approximations are currently being explored. An integral equation describing the structure of water molecules in terms of sticky interaction points is currently under development.[27,28] A theory based on a limited expansion in terms of two- and three-body correlation functions was developed to describe the hydration structure around nucleic acids[29] and proteins.[30] The latter approach provides a computationally inexpensive approximation, although the treatment may not be able to account for dielectric shielding properly because of the truncated expansion. There remains a need for an accurate and computationally simple theory able to realistically represent the solvation of polar molecules in liquid water.

In this work we present an integral equation theory to describe the essential structural features of liquid water around a polar molecule of arbitrary shape. In the present approach the fundamental quantities are the site-reduced average solvent densities $\langle\rho_\alpha(\mathbf{r})\rangle$ at all points $\mathbf{r}$, where α is an interaction site within the water solvent molecule. The integral equation is constructed on the basis of the density functional theory of nonuniform polyatomic liquids formulated by Chandler, McCoy, and Singer.[31] The integral equation reduces to the familiar RISM-HNC equation in the case of spherical solute.[15] All solvent effects and thermodynamic properties follow directly from the site-reduced average densities. The theory is formulated in section II. Applications and computational details are presented in section III. The approach is illustrated with the calculation of the hydration structure around a single water molecule (considered as a solute) and around a *N*-methylacetamide (NMA) molecule. The method could easily be extended to other polyatomic solvents (e.g., constituted of organic molecules). The results are discussed in section IV and followed by the conclusion (section V).

II. Theoretical Developments

To establish the formal basis of the theory, we consider an isolated molecular solute immersed in a polyatomic liquid of uniform density $\bar{\rho}$. It is assumed that a solvent molecule contains a number of interaction sites α. Owing to the presence of the solute, each interaction center α associated with the solvent molecule is affected by the perturbing potential $U_\alpha(\mathbf{r})$. For the sake of simplicity, the solute−solvent interaction is represented in terms of a superposition of radially symmetric 6-12 Lennard-Jones (LJ) and Coulomb electrostatic potential functions similar to those used in simulations based on standard biomolecular force fields[1]

$$U_\alpha(\mathbf{r}) = \sum_s u_{s\alpha}^{6\text{-}12}(|\mathbf{r}-\mathbf{r}_s|) + \sum_s \frac{q_s q_\alpha}{|\mathbf{r}-\mathbf{r}_s|} \tag{1}$$

where roman and Greek symbols indicate the solute and solvent sites, respectively. The LJ parameters and the partial charges are taken directly from standard biomolecular force fields.[32,33] In fact, the form of $U_\alpha(\mathbf{r})$ is not restrictive. Since there is no limit to the number of interaction sites inside the molecular solute, the treatment of a continuous ab initio charge distribution obtained from an electronic wave function is straightforward.[2,3,8−10]

We seek a simple and computationally tractable integral equation allowing the calculation of $\langle\rho_\alpha(\mathbf{r})\rangle$. Following the density functional theory for nonuniform polyatomic liquids of Chandler, McCoy, and Singer,[31] we consider the free energy density functional truncated to second order in intramolecular and intermolecular correlations

$$\beta A[\langle\rho_\alpha(\mathbf{r})\rangle] = \sum_\alpha \int d\mathbf{r}\, \langle\rho_\alpha(\mathbf{r})\rangle \ln\left[\frac{\langle\rho_\alpha(\mathbf{r})\rangle}{\bar{\rho}}\right] - \Delta\rho_\alpha(\mathbf{r}) + \beta U_\alpha(\mathbf{r})\langle\rho_\alpha(\mathbf{r})\rangle - \frac{1}{2}\sum_{\alpha\gamma}\int d\mathbf{r}\int d\mathbf{r}'\, \Delta\rho_\alpha(\mathbf{r})\bar{c}_{\alpha\gamma}(|\mathbf{r}-\mathbf{r}'|)\Delta\rho_\gamma(\mathbf{r}') \tag{2}$$

where $\beta = 1/k_B T$ and $\Delta\rho_\alpha(\mathbf{r}) = \langle\rho_\alpha(\mathbf{r})\rangle - \bar{\rho}$ is the deviation from the uniform density $\bar{\rho}$. The direct correlation function $\bar{c}_{\alpha\gamma}(|\mathbf{r}-\mathbf{r}'|)$ is defined in terms of the equilibrium site-site density susceptibility of the uniform unperturbed liquid

$$\bar{c}_{\alpha\gamma}(\mathbf{r}) = (\bar{\rho})^{-1}\delta_{\alpha\gamma}\delta(\mathbf{r}) - \chi_{\alpha\gamma}^{-1}(\mathbf{r}) \tag{3}$$

The solvent susceptibility is related to the density fluctuations of pair of sites $\chi_{\alpha\gamma}(\mathbf{r}-\mathbf{r}') = \langle\delta\rho_\alpha(\mathbf{r})\delta\rho_\gamma(\mathbf{r}')\rangle$, which can also be expressed in terms of the radial intramolecular and intermolecular site−site pair correlation functions $h_{\alpha\gamma}(r)$ of the pure unperturbed liquid as[34]

$$\chi_{\alpha\gamma}(r) = \bar{\rho}\omega_{\alpha\gamma}(r) + \bar{\rho}^2 h_{\alpha\gamma}(r) \tag{4}$$

For rigid solvent molecules, the function $\omega_{\alpha\gamma}(r)$ can be expressed in Fourier space as $\hat{\omega}_{\alpha\gamma}(k) = \sin(kl_{\alpha\gamma})/(kl_{\alpha\gamma})$ where $l_{\alpha\gamma}$ is the intramolecular distance between the interaction centers α and γ in the solvent molecule.

According to the free energy variational principle,[31] the average site density is obtained by minimization of the functional A with respect to the functions $\langle\rho_\alpha(\mathbf{r})\rangle$. This leads to the HNC-like integral equation

$$\langle\rho_\alpha(\mathbf{r})\rangle = \bar{\rho}\, e^{-\beta U_\alpha(\mathbf{r}) + \sum_\gamma \bar{c}_{\alpha\gamma} * \Delta\rho_\gamma(\mathbf{r})} \tag{5}$$

where the symbol $*$ represents a three-dimensional spatial convolution. The integral equation, eq 5, can be rewritten in a form more suitable for numerical calculations as a pair of coupled equations:

$$c_\alpha(\mathbf{r}) = e^{-\beta U_\alpha(\mathbf{r}) + h_\alpha(\mathbf{r}) - c_\alpha(\mathbf{r})} - h_\alpha(\mathbf{r}) + c_\alpha(\mathbf{r}) - 1 \tag{6}$$

and

$$\bar{\rho} h_\alpha(\mathbf{r}) = \sum_\gamma c_\gamma * \chi_{\gamma\alpha}(\mathbf{r}) \tag{7}$$

where $h_\alpha(\mathbf{r})$ is the solute−solvent site correlation function $h_\alpha(\mathbf{r}) \equiv [\Delta\rho_\alpha(\mathbf{r})/\bar{\rho} - 1]$ and $c_\alpha(\mathbf{r})$ is the solute−solvent site direct correlation function. Equations 6 and 7 are the main result of this article.

Even though eqs 6 and 7 resemble those of a simple mixture, intramolecular and intermolecular correlations and included through the solvent site−site susceptibility $\chi_{\alpha\gamma}$. The implications of the integral equation for the solvent structure around a solute of arbitrary shape may be easily understood. At short range, $\langle\rho_\alpha(\mathbf{r})\rangle \approx 0$ and the solvent molecules are excluded from the volume occupied by the solute because of the core repulsion. At large distances where the potential $U_\gamma(\mathbf{r})$ is weak relative to $k_B T$, the integral equation obeys the linear response[34]

$$\Delta\rho_\alpha(\mathbf{r}) \sim -\bar{\rho}\sum_\gamma \beta U_\gamma * \chi_{\gamma\alpha}(\mathbf{r}) \tag{8}$$

It follows that, by construction, eqs 6 and 7 can be thought of as a nonlinear interpolation between two important limits, incorporating both short- and long-range features of the three-

dimensional solvent structure around the solute. In particular, the dielectric response of liquid water arises from the long-range properties of the solvent susceptibility function $\chi_{\alpha\gamma}(\mathbf{r})$.[34] The present theory retains all the information about the solvent density around the molecular solute. In contrast, previous RISM theories were constructed only on the basis of the site−site solute−solvent radial pair distribution functions[15,22]

$$c_{s\alpha}(r) = e^{-\beta u_{s\alpha}^{6\text{-}12}(r)+h_{s\alpha}(r)-c_{s\alpha}(r)} - h_{s\alpha}(r) + c_{s\alpha}(r) - 1 \quad (9)$$

and

$$\bar{\rho}h_{s\alpha}(r) = \sum_{\gamma s'} \omega_{ss'}^{(u)} * c_{s'\gamma} * \chi_{\gamma\alpha}(r) \quad (10)$$

where $\omega_{ss'}^{(u)}$ is the intramolecular correlation function of the solute. In the special case of a simple monoatomic solute, $\omega^{(u)}(r) = \delta(r)$ and eqs 6 and 7 are equivalent to the radial RISM-HNC eqs 9 and 10. In the more general case of a solute of arbitrary shape, the present theory (3d-RISM-HNC) provides an extension to the radial RISM-HNC approximation in three dimensions.

III. Applications and Computational Details

The LJ parameters, geometry, and partial charges of water used in the calculations were taken from the TIP3P model.[32] The solvent susceptibility of bulk water was calculated on the basis of the standard RISM-HNC theory[14] and stored in **k**-space for the 3d-RISM-HNC calculations. Equations 6 and 7 were then used for calculating the average water density around the solute. As in our previous work,[24,26] a mapping of all functions of interest on three-dimensional discrete grid was used for the numerical solution. A cubic discrete grid of 128 points with a spacing of 0.225 Å, corresponding to an elementary cell of 28.8 Å, was used. The spatial convolutions $c_\gamma * \chi_{\gamma\alpha}(\mathbf{r})$ in eq 7 were calculated using a numerical three-dimensional fast Fourier transform (3d-FFT) procedure.[35] The electrostatic potentials were calculated directly in Fourier space as described previously.[26] No special renormalization procedure was necessary to treat the long-range interactions. As in previous work,[24,26] eqs 6 and 7 were solved self-consistently using an iterative procedure. Iterations were performed on the real-space direct correlation function. A mixing procedure analogous to that described previously was used in the initial steps of iteration;[26] no mixing was used after the initial steps. In the first stage, the direct correlation functions $c_\alpha(\mathbf{r})$ were calculated for the neutral solute (with all solute partial charges switched off). In the second stage, the solute charges were progressively switched on using a scaling parameter λ, increasing from 0 to 1 by increment of $\Delta\lambda = 0.01$. Finally, 40−100 iterations with $\lambda = 1$ were performed to reach convergence. The iterative procedure was repeated until the maximum change in the direct correlation functions $|c_\alpha^{(new)} - c_\alpha^{(old)}|$ over any grid points was less than 2.00×10^{-4}. The normalized radial distribution functions around the solute atoms were calculated explicitly in real space using the density $\rho_\alpha(\mathbf{r})$ in three dimensions.

The computational algorithm handling the solvent density in three dimensions was tested by comparing the results with those obtained with radial eqs 9 and 10 in the case of a positively charged spherical particle. (LJ parameters were $\sigma = 2.7165$ Å and $\epsilon = 0.152073$ kcal/mol.) The results (not shown) were almost indistinguishable from those obtained within the standard radial RISM-HNC equation, thereby validating the numerical implementation of the theory in three dimensions.

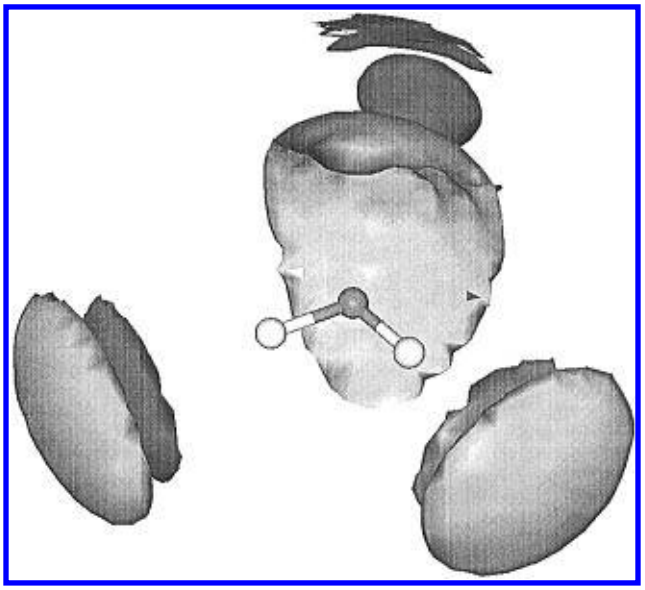

Figure 1. Molecular graphics representation of the average water oxygen and hydrogen densities surrounding a solute water molecule (eqs 6 and 7). The contours were chosen to illustrate the first hydration shell. The water hydrogen density is shown in light gray; the water oxygen density is shown in dark gray.

Two calculations were performed to test and illustrate the theory. In the first one a single water molecule was regarded as a solute dissolved in water. In the second calculation the solvation of *N*-methylacetamide (NMA) in the *trans* conformation was examined. The geometry, the Lennard-Jones (LJ) parameters, and the partial charges of NMA were the same as those used previously by Jorgensen.[33] The LJ parameters of the hydrogens in water and in NMA were set to nonzero values ($\sigma = 0.4$ Å and $\epsilon = 0.046$ kcal/mol) required for the stability of the integral equation.

IV. Results and Discussion

To illustrate the 3d-RISM-HNC theory, a water molecule was first considered as a solute. The average density of water oxygen and hydrogen calculated (in three dimensions) around one water molecule using eqs 6 and 7 are shown in Figure 1. There are oxygen density peaks followed by hydrogen peaks near the solute hydrogens. Correspondingly, there is a broad hydrogen density peak followed by a weaker oxygen density near the solute oxygen. The solvation structure is consistent with the main features expected for a hydrogen-bonding system. From the average solvent site density $\langle\rho_\alpha(\mathbf{r})\rangle$ the normalized solute−solvent site−site radial distribution functions were calculated. The results are shown in Figure 2 (solute H with solvent H, solute H with solvent O, solute O with solvent H, and solute O with solvent O). The radial distributions are qualitatively reasonable. However, it is observed that the radial distribution function of solvent oxygen around the solute hydrogen differs from the radial distribution function of solvent hydrogen around the solute oxygen. In an exact theory, these distribution functions should be identical by symmetry. The first solvent hydrogen peak is closer to the solute oxygen and, as a result, significantly higher than the corresponding solvent oxygen peak around the solute hydrogen. This is a well-documented deficiency observed also with the RISM theory[14] that is due to the lack of intramolecular correlation (see ref 31 for discussion). The intramolecular correlations are incorporated only to second order in the density functional theory given by eq 2, which allows the O−H solvent bond to stretch unrealistically. Although one possible route for solving this

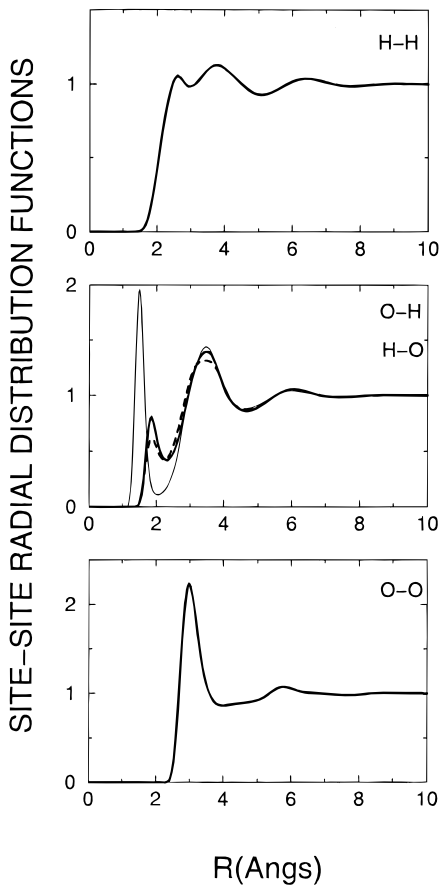

Figure 2. Site−site radial distribution function of water around the sites of a solute water molecule. In the central figure, the distribution of water oxygens around the hydrogens of the solute water is plotted with a dashed line. The distributions of water hydrogens around the oxygen calculated with and without bridge function are plotted with a bold and thin line, respectively.

problem is to use the full intramolecular contribution in eq 2,[31] for the sake of simplicity we introduced an empirical short-range function in eq 6, playing a role similar to the bridge function in the R-HNC theory.[12,36] It was assumed that, when the solvent water hydrogen forms a hydrogen bond with an electronegative solute atom, the combined LJ parameter σ for the pair of atoms is increased by 0.3 Å. The hydrogen radial distribution function after adjustment is shown by the dashed line in Figure 2. It is in much better agreement with the oxygen distribution function.

To illustrate the 3d-RISM-HNC theory in the case of a more complex solute, the density of water oxygen and hydrogen was calculated around one NMA molecule. The average water oxygen and hydrogen densities around NMA molecule are shown in Figure 3a. The solvation structure in three dimensions reflects the ability of the water molecules to form hydrogen bonds with NMA. Large density peaks of (water) oxygen and hydrogen are found in the vicinity of the amide hydrogen and of the carbonyl oxygen of NMA, respectively. Correspondingly, an adjacent region of high hydrogen and oxygen densities is observed, as expected based on the intramolecular structure of the water molecule. A third region of weaker water hydrogen density is observed in the neighborhood of the water oxygen peak surrounding the carbonyl oxygen of NMA. For comparison, a few solvent configurations, shown in Figure 3b, were extracted from molecular dynamics simulations to illustrate the hydration of NMA. It is observed that the hydrogen bonding of the water molecules to the C═O and N−H

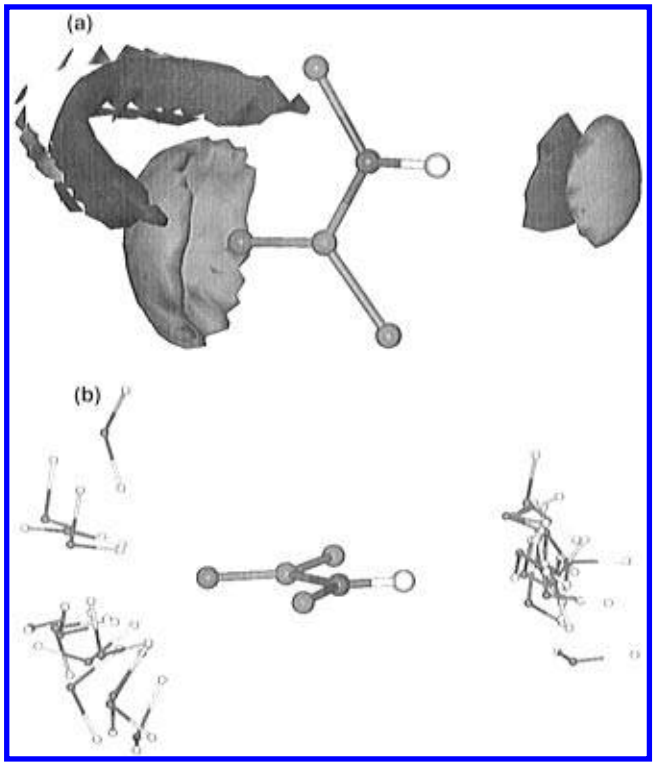

Figure 3. (a) Molecular graphics representation of the average water oxygen and hydrogen densities surrounding the NMA molecule as calculated from eqs 6 and 7. The contours were chosen to illustrate the first hydration shell around NMA. The water hydrogen density is shown in light gray; the water oxygen density is shown in dark gray. The N−H bond of NMA points toward the right and the C═O toward the left. (b) Superposition of a few snapshots of the nearest water molecules taken from a molecular dynamics simulation.

of NMA corresponds to the results obtained with the integral equation.

The normalized radial distribution of the water sites around NMA centers was calculated from the average density distribution in three dimensions. The radial distribution functions are shown in Figure 4. A molecular dynamics simulation of NMA in water was performed for comparison (the details of the simulation are given in the figure caption). The dashed line corresponds to results from the molecular dynamics simulation. The bold and thin solid lines correspond to the results of the integral equation with and without a simple bridge function as described above. As expected, the results of the integral equation and molecular dynamics simulation are in good accord except for the distribution of water hydrogen around the carbonyl oxygen. As in the case of the previous solute, introduction of a simple short-range correction improves the agreement with the simulation. The bridge function also affects slightly the oxygen distribution, since they are coupled via eq 7. The average nonbonded energies between the solute atoms and the solvent are given in Table 1. As expected, the interactions involving the carbonyl oxygen is not in very good agreement with the results of the simulation. The LJ is too positive (0.07 kcal/mol rather than −0.29 kcal/mol) and the electrostatic is too negative (−24.90 kcal/mol rather than −16.37 kcal/mol). However, the solvation energies calculated with the 3d-RISM-HNC corrected with a short-range bridge function are in much better agreement with the results from the simulation (e.g., the LJ and electrostatic contributions are −1.19 and −19.91 kcal/mol, respectively). The improved accord with the simulation suggests that quantitative accuracy for a large number of solutes could be achieved based on a limited empirical parametrization of bridge functions.

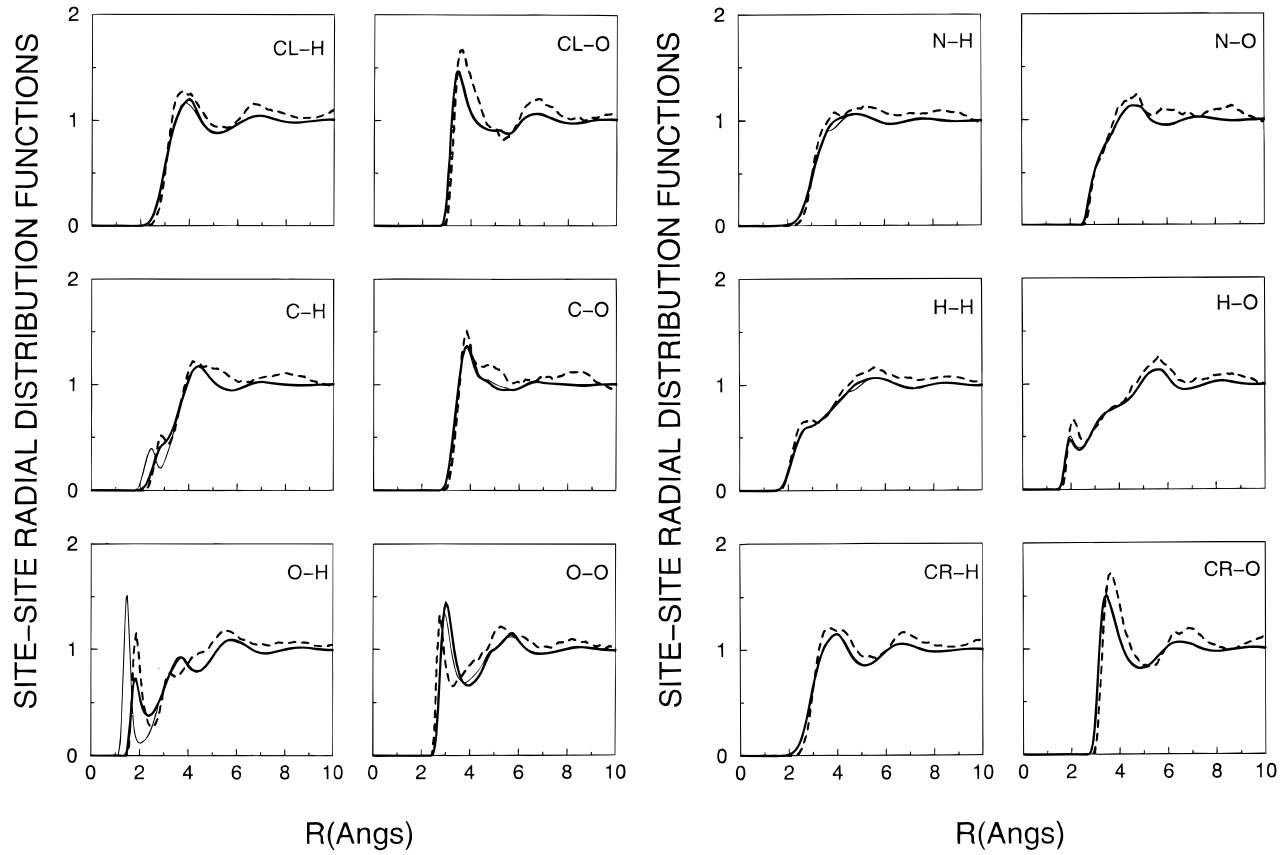

Figure 4. Site−site radial distribution functions of water oxygens and hydrogens around the atoms of NMA. The results of molecular dynamics are shown by dashed lines. The MD simulation was performed with 300 explicit TIP3P waters around the NMA molecule (the same conformation and parameters as in the integral equation calculations were used). The average distribution was calculated from a trajectory of Langevin dynamics of 300 ps with a friction constant applied to the oxygens corresponding to a relaxation time of 5 ps^{-1}. The spherical solvent boundary potential (SSBP) was used to mimic the behavior of an infinite bulk system.[37] The results of the present theory before and after the adjustment are shown by thin and bold solid lines, respectively.

TABLE 1: Water−NMA Nonbonded Interaction Energy (kcal/mol)

	3d-RISM-HNC integral equation					
	no bridge		with bridge		simulation	
atom	LJ	elec	LJ	elec	LJ	elec
CL	−1.46	0.00	−1.48	0.00	−2.40	0.00
C	−2.04	8.23	−2.06	8.73	−2.33	3.87
O	0.07	−24.90	−1.19	−19.01	−0.29	−16.37
N	−1.40	0.96	−1.45	−2.11	−1.73	3.33
CR	−1.49	0.40	−1.50	1.32	−2.49	−0.58
H	−0.10	−5.76	−0.09	−2.90	−0.11	−6.32
total	−6.42	−21.07	−7.77	−14.00	−9.35	−16.06

The electrostatic solvent reaction field potential is defined in terms of the average density of solvent sites $\langle\rho_\alpha(\mathbf{r})\rangle$ as

$$\psi^{(\mathrm{rf})}(\mathbf{r}) = \int d\mathbf{r}' \frac{1}{|\mathbf{r}-\mathbf{r}'|} \sum_\alpha q_\alpha \langle\rho_\alpha(\mathbf{r}')\rangle \qquad (11)$$

The reaction field was first calculated in **k**-space and then inverted back to real space using a three-dimensional Fourier transform. The solvent reaction field in the plane of NMA molecule is shown in Figure 5 as a contour plot. The regions where the potential is positive are shaded. The potential is generally positive on the side of the carbonyl oxygen. There are oscillations altering the pattern of potential from the simple dipolar one. The main features of the solvation of NMA are consistent with its polarity. The dipole of NMA points roughly from the carbonyl oxygen to the amide hydrogen, and the water molecules in the first hydration shell are polarized in the opposite direction. The effect of solvent is thus qualitatively similar to that of a continuum electrostatic reaction field, i.e., the permanent dipole of the solute polarizes the solvent, which in turn creates an electric field in the opposite direction.[5,10] However,

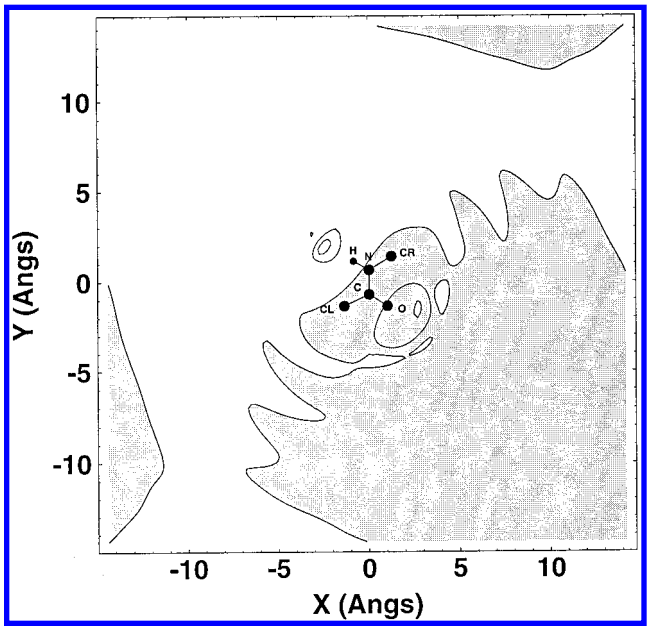

Figure 5. Electrostatic potential caused by the solvent polarization $\psi^{(\mathrm{rf})}$ in the plane of the NMA molecule. The potential was calculated in atomic units e/Å. The contours are plotted in the range from −0.6 to 0.3 with increments of 0.1. The shaded regions are where the potential is positive.

a simple continuum electrostatic description of the solvent[6] would be unable to incorporate the microscopic structural details observed in the hydration shell around NMA (see Figures 3 and 4).

V. Summary

The interest of the present 3d-RISM-HNC integral equation lies in the fact that the average solvent site density $\langle \rho_\alpha(\mathbf{r}) \rangle$ is determined at all points **r**. We believe that this three-dimensional extension to the RISM-HNC equation represents a significant theoretical and computational advance. It makes it possible to take into account essential structural solvent features that are beyond the limitations of continuum models of solvation. At the same time the computational cost is more modest than that of computer simulations. One particularly important aspect of the theory is its ability to incorporate the formation of solute−solvent hydrogen bonds. To achieve quantitative accuracy, simple bridge functions[36] will be parametrized empirically. Further development of the theory will be necessary to evaluate the solvation free energy. Future application of the 3d-RISM-HNC equation will include the treatment of solvent effects in ab initio calculations as well as in biomolecular simulations.

Acknowledgment. Discussions with Rich Friesner are gratefully acknowledged. This work was supported by NSERC. B.R. is a MRC research fellow.

References and Notes

(1) Brooks, C. L., III; Karplus, M.; Pettitt, B. M. Proteins. A theoretical perspective of dynamics, structure and thermodynamics. In *Advances in Chemical Physics*; Prigogine, I., Rice, S. A., Eds.; John Wiley & Sons: New York, 1988; Vol. LXXI.
(2) Gao, J.; Xia, X. *Science* **1992**, *258*, 631.
(3) Gao, J. *J. Am. Chem. Soc*. **1994**, *116*, 9324.
(4) Kirkwood, J. G. *J. Chem. Phys*. **1934**, *2*, 351.
(5) Onsager, L. *J. Chem. Phys*. **1936**, *58*, 1468−1493.
(6) Sharp, K. A.; Honig, B. *Annu. Rev. Biophys. Biophys. Chem*. **1990**, *19*, 301−332.
(7) Still, W. C.; Tempczyk, A.; Hawley, R. C.; Hendrickson, T. *J. Am. Chem. Soc*. **1990**, *112*, 6127.
(8) Klamt, A.; Schüürmann, G. *J. Chem. Soc., Perkin Trans*. **1993**, *2*, 799.
(9) York, D. M.; Lee, T. S.; Yang, W. *J. Am. Chem. Soc*. **1996**, *118*, 10940−10941.
(10) Cramer, C. J.; Truhlar, D. G. Continuum solvation models: classical and quantum mechanical implementations. In *Reviews in computational chemistry*; Lipkowitz, K. B., Ed.; VCH: New York, 1995.
(11) Hansen, J. P.; McDonald, I. R. *Theory of Simple Liquids*; Academic Press: London, 1976.
(12) Fries, P. H.; Patey, G. N. *J. Chem. Phys*. **1985**, *82*, 429−440.
(13) Chandler, D.; Andersen, H. C. *J. Chem. Phys*. **1972**, *57*, 1930−1937.
(14) Hirata, F.; Rossky, P. J. *Chem. Phys. Lett*. **1981**, *83*, 329−334.
(15) Pettitt, B. M.; Rossky, P. J. *J. Chem. Phys*. **1986**, *84*, 5836−5844.
(16) Yu, H. A.; Karplus, M. *J. Chem. Phys*. **1988**, *89*, 2366.
(17) Pettitt, M. B.; Karplus, M. *Chem. Phys. Lett*. **1985**, *121*, 194−201.
(18) Pettitt, M. B.; Karplus, M.; Rossky, P. J. *J. Phys. Chem*. **1986**, *90*, 6335−6345.
(19) Pettitt, M. B.; Karplus, M. *Chem. Phys. Lett*. **1987**, *136*, 383−386.
(20) Lau, W. F.; Pettitt, B. M. *Biopolymers* **1987**, *26*, 1817−1831.
(21) Ramé, G.; Lau, W. F.; Pettitt, B. M. *Int. J. Pept. Protein Res*. **1990**, *35*, 315−327.
(22) Lee, P. H.; Maggiora, G. M. *J. Phys. Chem*. **1993**, *97*, 10175−10185.
(23) Perkyns, J. S.; Pettitt, B. M. *Chem. Phys. Lett*. **1992**, *190*, 626−630.
(24) Beglov, D.; Roux, B. *J. Chem. Phys*. **1995**, *103*, 360−364.
(25) Ikeguchi, M.; Doi, J. *J. Chem. Phys*. **1995**, *103*, 5011−5017.
(26) Beglov, D.; Roux, B. *J. Chem. Phys*. **1996**, *104*, 8678−8689.
(27) Liu, Y.; Ichiye, T. *Chem. Phys. Lett*. **1994**, *231*, 380−386.
(28) Hyun, J.-K.; Babu, C. S.; Ichiye, T. *J. Chem. Phys*. **1995**, *99*, 5187−5185.
(29) Hummer, G.; Soumpasis, D. M. *Phys. Rev. E* **1994**, *50*, 5085−5095.
(30) García, A. E.; Hummer, G.; Soumpasis, D. M. *Biophys. J*. **1997**, *72*, (2), A104.
(31) Chandler, D.; McCoy, J. D.; Singer, S. J. *J. Chem. Phys*. **1996**, *85*, 5971.
(32) Jorgensen, W. L.; Chandraskhar, J.; Madura, J. D.; Impey, R. W.; Klein, M. L. *J. Chem. Phys*. **1983**, *79*, 926−935.
(33) Jorgensen, W. L.; Gao, J. *J. Am. Chem. Soc*. **1988**, *110*, 4212−4216.
(34) Chandler, D. The equilibrium theory of polyatomic fluids. In *The Liquid State of Matter: Fluids, Simple and Complex*; Montroll, E. W., Lebowitz, J. L., Eds.; North-Holland: Amsterdam, 1982.
(35) Press, W. H.; Flannery, B. P.; Teukolsky, S. A.; Vetterling, W. T. *Numerical Recipes*; Cambridge University Press: Cambridge, 1990.
(36) Lado, F.; Foiles, S. M.; Ashcroft, N. W. *Phys. Rev. A* **1983**, *28*, 2374−2379.
(37) Beglov, D.; Roux, B. *J. Chem. Phys*. **1994**, *100*, 9050−9063.